



# Spatial-temporal evolution patterns and drivers of PM<sub>2.5</sub> chemical fraction concentrations in China over the past 20 years

Chao He<sup>1,2</sup> · Bin Li<sup>1,2</sup> · Xusheng Gong<sup>3</sup> · Lijun Liu<sup>1,2</sup> · Haiyan Li<sup>4</sup> · Lu Zhang<sup>5</sup> · Jiming Jin<sup>1,2</sup>

Received: 2 February 2023 / Accepted: 18 July 2023 / Published online: 22 July 2023  
© The Author(s), under exclusive licence to Springer-Verlag GmbH Germany, part of Springer Nature 2023

## Abstract

The quantitative assessment of the spatial and temporal variability and drivers of fine particulate matter (PM<sub>2.5</sub>) fraction concentrations are important for pollution control and public health preservation in China. In this study, we investigated the spatial temporal variation of PM<sub>2.5</sub> chemical component based on the PM<sub>2.5</sub> chemical component datasets from 2000 to 2019 and revealed the driving forces of the differences in the spatial distribution using geodetector model (GD), multi-scale geographically weighted regression model (MGWR), and a two-step clustering approach. The results show that: the PM<sub>2.5</sub> chemical fraction concentrations show a trend of first increasing (2000–2007) and then decreasing (2007–2019). From 2000 to 2019, the change rates of PM<sub>2.5</sub>, organic matter (OM), black carbon (BC), sulfates (SO<sub>2</sub>– 4), ammonium (NH<sub>4</sub><sup>+</sup> 4), and nitrates (NO<sub>3</sub><sup>–</sup> 3) were –0.59, –0.23, –0.07, –0.15, –0.02, and 0.04 μg/m<sup>3</sup>/yr in the entirety of China. The secondary aerosol (i.e., SO<sub>2</sub>– 4, NO<sub>3</sub><sup>–</sup> 3, and NH<sub>4</sub><sup>+</sup> 4; SNA) had the highest fraction in PM<sub>2.5</sub> concentrations (55.6–68.1% in different provinces), followed by OM and BC. Spatially, North, Central, and East China are the regions with the highest PM<sub>2.5</sub> chemical component concentrations in China; meanwhile, they are also the regions with the most significant decrease in PM<sub>2.5</sub> chemical fraction concentrations. The GD and MGWR model shows that among all variables, the number of enterprises, disposable income, private car ownership, and the share of secondary industry non-linearly enhance the differences in the spatial distribution of PM<sub>2.5</sub> component concentrations. Electricity consumption has the strongest influence on NH<sub>4</sub><sup>+</sup> 4 emissions in Northwest China and BC and OM emissions in Northeast China.

**Keywords** PM<sub>2.5</sub> chemical fraction · Spatiotemporal variations · Driving factors · MGWR · China

## Introduction

Fine particulate matter (PM<sub>2.5</sub>) is a complex mixture of multiple sources, including sulfates (SO<sub>2</sub>– 4), nitrates (NO<sub>3</sub><sup>–</sup> 3), ammonium (NH<sub>4</sub><sup>+</sup> 4), black carbon aerosols (BC), organic carbon (OC), Organic matter (OM), crustal elements, and water (Sun et al. 2015). Long-term exposure to high concentrations of PM<sub>2.5</sub> not only entails potential risks to socioeconomic development and population health (Apte et al. 2018), but some components of PM<sub>2.5</sub> (e.g., sulfate, organic carbon, and black carbon) affect global climate change by contributing to global energy emission systems (Cohen et al. 2017; Jbaily et al. 2022; Liu et al. 2009; Xu et al. 2022). Furthermore, high PM<sub>2.5</sub> concentrations may also trigger visibility degradation or lead to extreme haze events (Lelieveld et al. 2015; Ming et al. 2017).

Measuring the spatial and temporal evolution and historical trends of PM<sub>2.5</sub> fractions is the basis for exploring population health risks and future control policy assessment. In

Responsible Editor: Gerhard Lammel

✉ Lu Zhang  
541462161@qq.com

<sup>1</sup> College of Resources and Environment, Yangtze University, Wuhan 430100, China

<sup>2</sup> Hubei Key Laboratory of Petroleum Geochemistry and Environment, Yangtze University, Wuhan 430100, China

<sup>3</sup> School of Nuclear Technology and Chemistry & Biology, Hubei University of Science and Technology, Xianning 437100, China

<sup>4</sup> Shanghai Environmental Protection Co., Ltd., Shanghai 200233, China

<sup>5</sup> State Key Laboratory of Freshwater Ecology and Biotechnology, Institute of Hydrobiology, Chinese Academy of Sciences, Wuhan 430072, China

the past decades, numerous studies on the characteristics and historical trends of  $PM_{2.5}$  fractions in China have typically relied on measured data from several sites or regional simulations based on chemical transport models (CTMs) (Zheng et al. 2021). For example, Liang et al. (2019) evaluated the seasonal dynamics of  $PM_{2.5}$  composition and chemical characteristics in Zhuhai from 2015 to 2016 using a 2-medium-volume sampler, while explaining the potential sources of  $PM_{2.5}$  composition. Geng et al. (2017) integrated aerosol optical thickness (AOD) data and GEOS-Chem chemical transport model, investigated the spatial and temporal characteristics of  $PM_{2.5}$  chemical composition concentrations in major cities from 2005 to 2012 in China, and explained the driving forces of spatial heterogeneity. Furthermore, Sun et al. (2015) relied on measured data from several stations or used chemical transport models to characterize the variability of  $PM_{2.5}$  fractions in different regions of China; Liu et al. (2018) studied the variations of  $PM_{2.5}$  fraction concentrations in urban and background areas in China from 2012 to 2014 based on the “Campaign on Atmospheric Aerosol Research” network of China (CARE-China).

The aforementioned have significant implications for understanding the variation of  $PM_{2.5}$  component concentrations in China at different spatial and temporal scales. However, there is growing evidence that individual cities or short-term  $PM_{2.5}$  fraction measurements are insufficient to support comprehensive national analyses or health impact studies, because air quality problems are usually regional issues and are influenced by many different factors, social and natural factors such as socioeconomic factors, anthropogenic emissions, and natural emissions (Chen et al. 2020; Guo et al. 2017). CTMs are important for understanding  $PM_{2.5}$  pollution levels, drivers, and potential sources at different spatial and temporal scales (Feng et al. 2015). However, it is worth noting that CTMs were originally developed in other regions with different pollution levels compared to China (Wei et al. 2021). The application of these models in China might pose some problems with missing precursors and formation mechanisms of secondary organic aerosols and the lack of heterogeneous reactions, which may eventually lead to the underestimation of sulfate in haze events (Geng et al., 2017). Therefore, more information is needed to alleviate these problems and improve the simulations of historical  $PM_{2.5}$  chemical compositions.

Currently, a new dataset was being developed by Tsinghua University as a cooperative effort among several institutions and teams, namely, the Tracking Air Pollution in China (TAP) Data (Geng et al. 2021). The purpose was to establish a multi-scale database of near real time aerosol and gaseous pollutant concentrations in China and provide the necessary support for pollution characterization analysis (Zhao et al. 2022). At present, this dataset provides  $PM_{2.5}$  chemical component concentrations in

China from 2000 to 2019. Compared with the previous  $PM_{2.5}$  component dataset simulated by CTMs, the TAP dataset is generated based on machine learning algorithms and multi-source data information. Meanwhile, the TAP dataset integrates ground observation data, satellite remote sensing information, high-resolution emission inventory, air quality model simulation, and other multi-source information to construct a multi-source data fusion (Xiao et al. 2021). To our knowledge, the TAP dataset is by far the most accurate, largest-coverage, and longest time-span  $PM_{2.5}$  component dataset available and has been validated and effectively applied on a regional scale (Zhao et al. 2022).

This study investigated the spatiotemporal patterns, variation trends, and social drivers of  $PM_{2.5}$  chemical fraction in China using the newly released national-scale  $PM_{2.5}$  chemical fraction concentration dataset from 2000 to 2019. The specific objectives were (1) to reveal the spatial-temporal characteristics of  $PM_{2.5}$  chemical fraction concentrations in China from 2000 to 2019 using spatial and trend analyses and (2) to explore the spatial differences in the effects of major socioeconomic factors on  $PM_{2.5}$  chemical fraction concentrations based on the multi-scale weighted regression MGWR model and GD model.

## Materials and methods

### Study area

This study focuses on China mainland, which contains 31 provinces. Based on the social, natural, economic, and human environment, these 31 regions were further categorized into seven geo-administrative regions, including North China (NC, Beijing, Tianjin, Hebei, Shanxi, and Inner Mongolia), South China (SC, Guangdong, Guangxi, and Hainan), East China (EC, Shanghai, Anhui, Fujian, Jiangsu, Jiangxi, Shandong, and Zhejiang), Central China (CC, Henan, Hunan, and Hubei), Southwest China (SW, Yunnan, Guizhou, Sichuan, Chongqing, and Tibet), Northwest China (NW, Shaanxi, Gansu, Ningxia, Qinghai, and Xinjiang), and Northeast China (NE, Heilongjiang, Jilin, and Liaoning) (Fig. 1a) (Gong et al. 2018). Figure 1b shows the frequency statistical histogram of  $PM_{2.5}$ , black carbon (BC), organic matter (OM), ammonium ( $NH_4^+$ ), nitrate ( $NO_3^-$ ), and sulfate ( $SO_4^{2-}$ ) concentrations in 31 provinces of China from 2000 to 2019. The statistical results show that the concentrations of  $PM_{2.5}$ , BC, OM,  $NH_4^+$ ,  $NO_3^-$ , and  $SO_4^{2-}$  were basically showed a positive distribution. Meanwhile, the concentrations of  $PM_{2.5}$ , BC, OM,  $NH_4^+$ ,  $NO_3^-$  and  $SO_4^{2-}$  were mainly distributed between 30 and 50, 1 and 2.5, 6 and 12, 0 and 7, 2 and 8, and 4 and  $10\mu g/m^3$ .

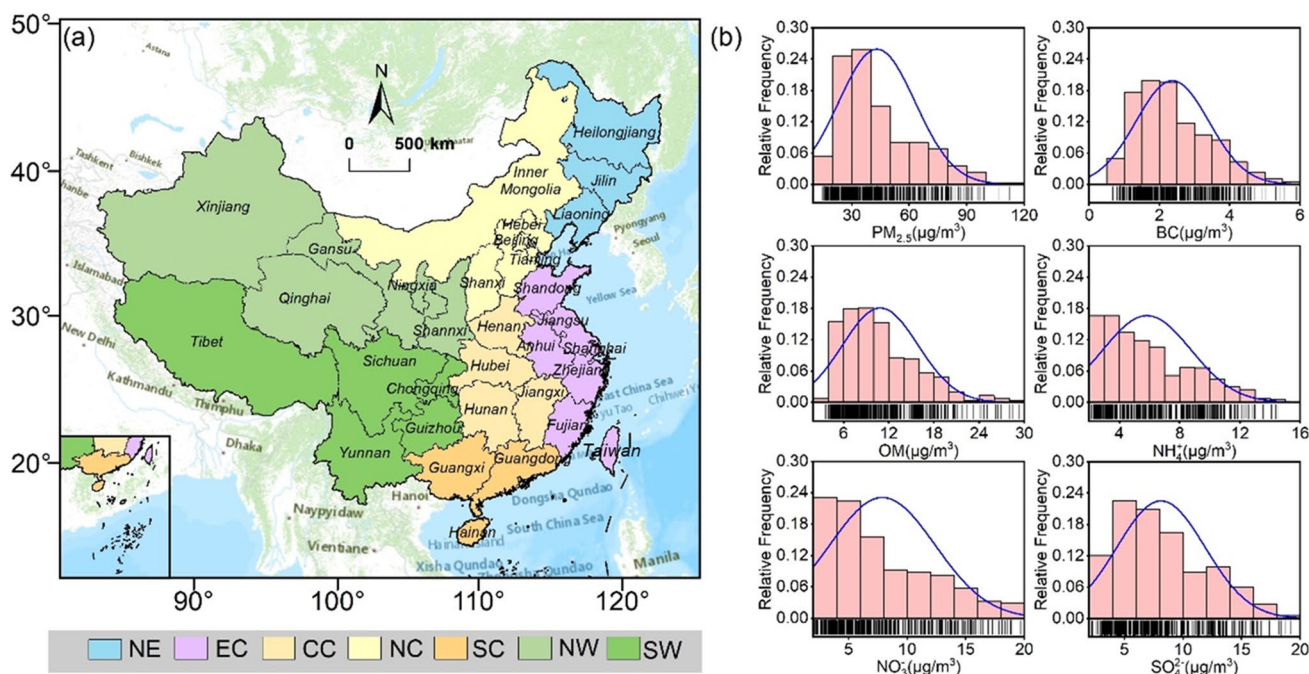


**Fig. 1** The spatial distribution of the 31 provinces (a) and the frequency statistical histogram of  $PM_{2.5}$ , BC, OM,  $NH_4^+$ ,  $NO_3^-$  and  $SO_2-4$  concentrations (b)

**Data sources**

The annual average  $PM_{2.5}$ , BC, OM,  $NH_4^+$ ,  $NO_3^-$ , and  $SO_2-4$  concentrations in 31 provinces of China from 2000 to 2019 were obtained from the Tracking Air Pollution

in China (TAP) datasets (<http://tapdata.org.cn/>). The  $PM_{2.5}$  component concentration in the TAP dataset is the result of coupling the current advanced machine learning algorithm and the atmospheric chemical transport model; the model has an average out-of-bag cross-validation  $R^2$  of 0.83 in different years, which is comparable to the results of other studies (Geng et al. 2017). Its high accuracy and high coverage characteristics can provide basic data support for air pollution health effects, clean air policy assessment, and other related scientific research and environmental management work (Liu et al. 2022). To quantitatively investigate the impact of socio-economic factors on  $PM_{2.5}$  and its chemical components, we obtained eight socio-economic indicators such as the number of enterprises (NOE), disposable income (DI), gross domestic product (GDP), and electricity consumption (EC) of 31 provinces in China from 2000 to 2019 from the EPS database (<https://www.epsnet.com.cn/index.html#/Index>). The specific information about the basic and statistical description of the main socio-economic indicators can be found in Table 1 and Table.S1.

**MAKESENS mode**

To evaluate the trends of  $PM_{2.5}$  chemical fractions in China, we introduced an integrated method called Mann–Kendall trend test, which is based on several conditional functions (Partal and Kahya, 2006). The greatest advantage of the MAKESENS model is that it assumes no distribution of the data; therefore, outliers and missing values do not significantly affect the model results. Prior to the trend test, the Mann-Kendall test was first performed on the time series data. When the time series of the study data is less than 10, the MAKESENS model uses the *S-test*; conversely, when it is above 10, the model uses the *Z-test*. The time period of this study is 2000-2019; therefore, the calculations for this

**Table 1** The list of main socio-economic variables

Variable	Abbreviation	Unit
Number of enterprises	NOE	Number
Disposable income	DI	Yuan
Gross domestic product	GDP	100 million yuan
NOx emission	NOx	tons
Electricity consumption	EC	Billion kWh
Private vehicle ownership	PVO	10000 vehicles
Percentage of secondary industry	SIS	%
$SO_2$ emission	$SO_2$	tons

study were based on the *Z-test*. We then used Sen's method to calculate the linear trend of PM<sub>2.5</sub> chemical fraction concentration. The detailed calculation procedure of the *Z-test* and Sen's method can be found in Equations (1)–(5):

$$S = \sum_{k=1}^{n-1} \sum_{j=k+1}^n \operatorname{sgn}(x_j - x_k) \quad (1)$$

$$Z = \begin{cases} \frac{S-1}{\sqrt{\operatorname{VAR}(S)}} & \text{if } S > 0 \\ 0 & \text{if } S = 0 \\ \frac{S+1}{\sqrt{\operatorname{VAR}(S)}} & \text{if } S < 0 \end{cases} \quad (2)$$

$$\operatorname{VAR}(S) = \frac{1}{18} \left[ n(n-1)(2n+5) - \sum_{p=1}^q t_p(t_p-1)(2t_p+5) \right] \quad (3)$$

$$Q = \frac{x_j - x_k}{j - k} \quad (4)$$

$$Q = \begin{cases} Q_{\lfloor (N+1)/2 \rfloor}, & \text{if } N \text{ is odd} \\ \frac{1}{2} \left( Q_{\lfloor N/2 \rfloor} + Q_{\lfloor (N+1)/2 \rfloor} \right), & \text{if } N \text{ is even} \end{cases} \quad (5)$$

where  $n$  is the span of the time series, where  $n=20$ ;  $x_k$  and  $x_j$  are the annual average concentrations of PM<sub>2.5</sub> fraction in year  $k$  and year  $j$ , respectively ( $j>k$ );  $S$  is the orientation of the trend of the annual average concentration of PM<sub>2.5</sub> fraction;  $Z$  is used to assess the existence of a statistically significant trend;  $q$  is the number of tied groups and  $t_p$  is the number of data values in the  $p^{\text{th}}$  group; and  $Q$  is the trend of the annual average concentration of PM<sub>2.5</sub> fraction, when  $Q>0$ , the annual average concentration of PM<sub>2.5</sub> fraction is an increasing trend, and when  $Q<0$ , the annual average concentration of pollutants is a decreasing trend.

## Geodetector

The geodetector (GD) is an effective instrument to examine the spatial heterogeneity of a univariate factor and the coupling of multiple factors, which is composed of four parts: factor detection, risk detection, interaction detection, and ecological detection. In this work, the factor detection and interaction detection modules of the GD are used to detect quantitatively whether the driving factor affects the spatial heterogeneity of PM<sub>2.5</sub> component changes and to estimate the extent of the influence of the factor. The detailed calculation process of factor detection

and interaction detection in the GD is described in Wang et al. (2016).

## Multi-scale geographically weighted regression

In this study, the multi-scale geographically weighted regression (MGWR) model was used to investigate the spatial differences in the effects of the various socioeconomic factors on PM<sub>2.5</sub> components. Compared with the classical geographically weighted regression model (GWR), the MGWR was a flexible regression model (Tran et al. 2022). Each regression coefficient was obtained based on local regression, and the bandwidth is specific (Liu et al. 2021). In addition, the GWR model uses weighted least squares in the fitting operation, while the MGWR model was equivalent to a generalized additive model (GAM), which could perform regression analysis on spatial variables with linear or nonlinear relationships, and was also an effective tool for dealing with various complex nonlinear relationships of spatial variables (Oshan et al. 2019). Assuming that there are  $n$  observations, for observation  $i \in \{1, 2, 3, \dots, n\}$  at location  $(U_i, V_i)$ , the MGWR were calculated as follows (Fotheringham et al. 2017):

$$y_i = \beta_0(U_i, V_i) + \sum_j j\beta_{bwj}(U_i, V_i)X_{ij} + \varepsilon_i \quad (6)$$

where  $y_i$  is the response variable PM<sub>2.5</sub> or chemical composition concentration,  $\beta_0(U_i, V_i)$  is the intercept,  $X_{ij}$  is the  $j^{\text{th}}$  predictor variable  $i$ ,  $\beta_{bwj}(U_i, V_i)$  is the  $j^{\text{th}}$  coefficient,  $bwj$  in  $\beta_{bwj}$  indicates the bandwidth used for calibration of the  $j^{\text{th}}$  conditional relationship, and  $\varepsilon_i$  is the error term. In addition, the spatial kernel function type selected during the model operation is bisquare, the bandwidth search type is golden, and the model parameter initialization type takes GWR estimation as the initial estimation model. The detailed procedures of MGWR model construction and validation in this study can be found in supplementary information (SI).

## Two-step cluster

The MGWR model provides a large number of local regression coefficients. To better characterize the spatial distribution of these local regression coefficients, we performed a spatial clustering of these local regression coefficients with a two-step clustering method. A two-step cluster is an effective clustering approach that can be used to cluster both continuous and dispersed variables. In this study, a two-step cluster can divide provinces into different categories according to the correlations between different drivers. After clustering, there are similarities in the impact



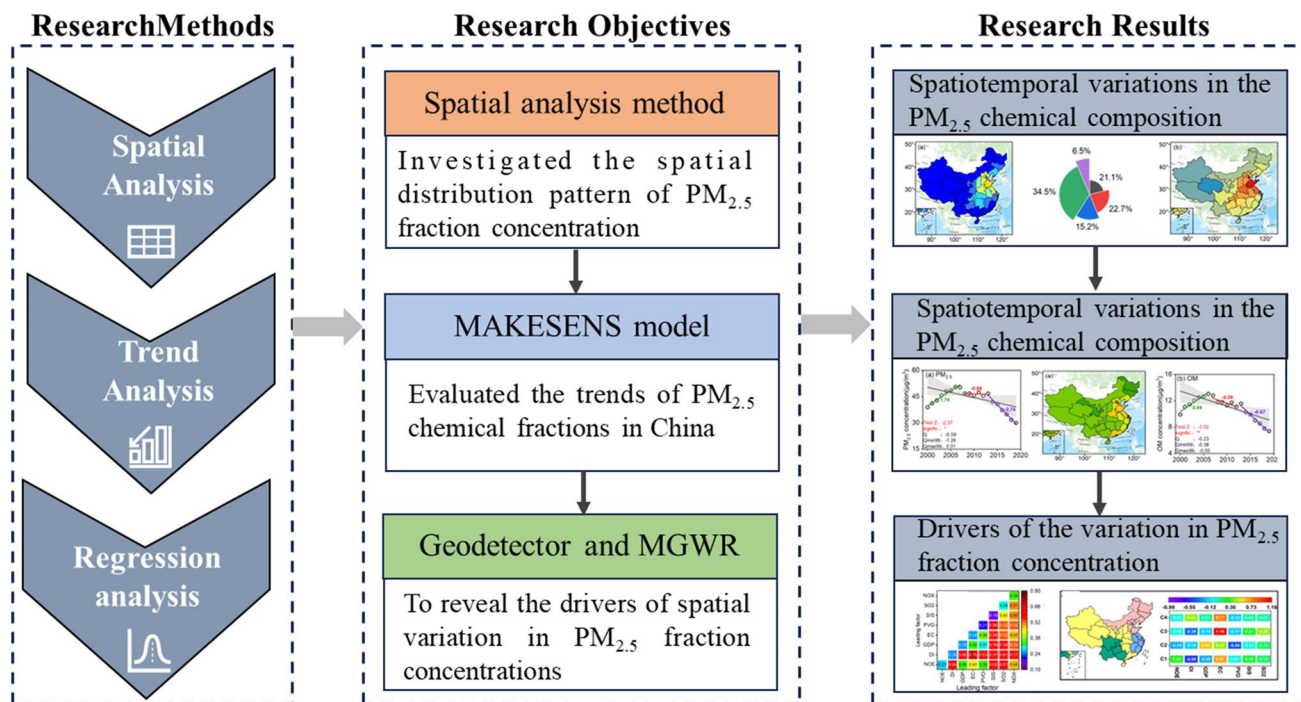


Fig. 2 Research framework

of social drivers in regions that are classified in the same category. A more detailed description of the two-step clustering method can be found in the research of Qin et al. (2019) and Yu et al. (2012).

**Research framework**

This study employed spatial analysis methods, MAKES-ENS mode, GD model, MGWR model, and two-step clustering to analyze the spatial patterns, trends, and drivers of PM<sub>2.5</sub> fraction concentrations in China during 2000–2019. First, we used the spatial analysis module in ArcGIS10.8 software to quantitatively investigate the differences in the spatial distribution of PM<sub>2.5</sub> component concentrations in China and used mathematical and statistical methods to statistically measure the proportion of different PM<sub>2.5</sub> component concentrations to PM<sub>2.5</sub> concentrations. Second, we analyzed the temporal and spatial variation characteristics of PM<sub>2.5</sub> component concentrations using the MAKESENS model in both temporal and spatial dimensions; Finally, we used GD model to reveal the interactive effects of different socio-economic factors on PM<sub>2.5</sub> component concentrations and analyzed the spatial differences in the influence of different socio-economic factors on PM<sub>2.5</sub> component concentrations using the MGWR model and the two-step clustering method. Figure 2 shows the research framework of this paper.

**Results**

**Spatiotemporal variations in the PM<sub>2.5</sub> chemical composition**

Figure 3 presents the mass concentrations of PM<sub>2.5</sub> and species in 31 provinces over China. Generally, the 20-year average 31 province concentrations of PM<sub>2.5</sub>, SO<sub>2</sub>– 4, NO– 3, NH<sub>4</sub><sup>+</sup> 4, OM and BC were 43.12 (18.74–88.20) μg/m<sup>3</sup>, 8.12 (2.89–14.74) μg/m<sup>3</sup>, 7.89 (2.66–17.69) μg/m<sup>3</sup>, 5.83 (2.34–11.89) μg/m<sup>3</sup>, 10.88 (4.53–23.1) μg/m<sup>3</sup>, and 2.37 (0.92–4.50) μg/m<sup>3</sup>, respectively, from 2000 to 2019. The range in parentheses represents the maximum and minimum annual average concentrations in 31 provinces. Spatially, the average concentrations of PM<sub>2.5</sub>, SO<sub>2</sub>– 4, NO– 3, NH<sub>4</sub><sup>+</sup> 4, OM and BC had significant spatial heterogeneity. The higher concentrations of PM<sub>2.5</sub>, SO<sub>2</sub>– 4, NO– 3, NH<sub>4</sub><sup>+</sup> 4, OM and BC were mainly distributed in Beijing–Tianjin–Hebei, Central China and East China, which were densely populated, economically developed and industrially concentrated. Meanwhile, these areas were also the areas with the most serious particulate matter pollution (PM) in China. In contrast, the lower concentrations of PM<sub>2.5</sub>, SO<sub>2</sub>– 4, NO– 3, NH<sub>4</sub><sup>+</sup> 4, OM and BC were mainly distributed in northwest and south China with low PM pollution.

Figure 4 summarizes the average PM<sub>2.5</sub> speciation for 31 provinces across China from 2000 to 2019. In general,

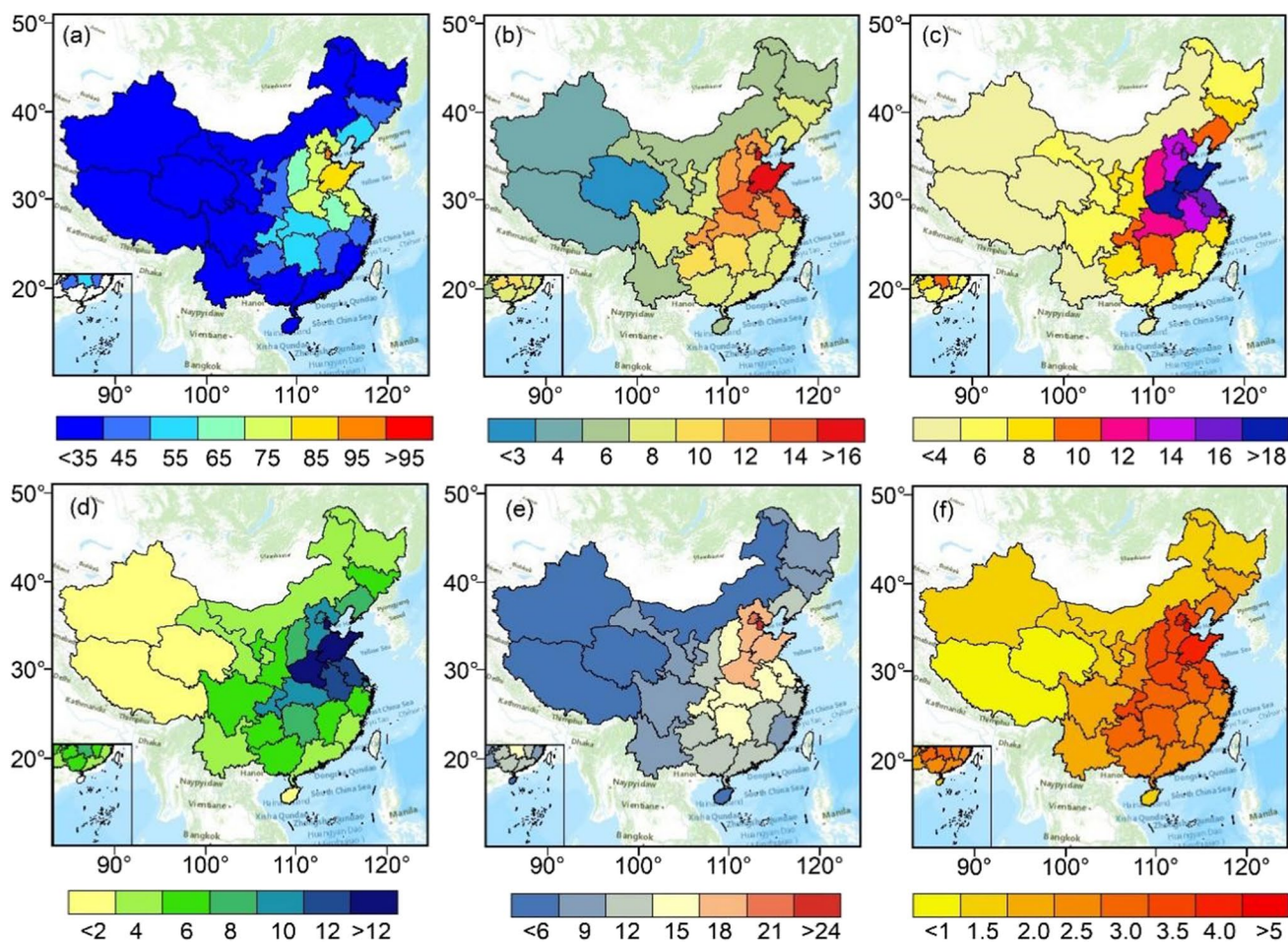


**Fig. 3** Spatial distribution of average  $PM_{2.5}$  (a),  $SO_2-4$  (b),  $NO_3-3$  (c),  $NH_4+4$  (d), OM (e), and BC (f) concentrations in China from 2000 to 2019. The units of  $PM_{2.5}$ ,  $SO_2-4$ ,  $NO_3-3$ ,  $NH_4+4$ , OM and BC concentration are all  $\mu g/m^3$

SNA ( $SO_2-4$ ,  $NO_3-3$ , and  $NH_4+4$ ) were major components of  $PM_{2.5}$  over Chinese provinces, which contributed 55.6 (Hainan)–68.1% (Jiangsu) of the  $PM_{2.5}$  concentrations in the 31 provinces. The regions with higher average SNA fraction were mainly distributed in Jiangsu (68.1%), Anhui (67.5%), Shandong (67.3%), and Henan (66.8%), and the areas with lower average SNA fraction were mainly distributed in Tianjin (59.7%), Guangxi (59.6%), and Gansu. OM was also an important component in  $PM_{2.5}$ , with averaged fractions of 26.4% (Jiangsu)–36.2% (Hainan). More than 70% of the provinces had OM fraction higher than 30.0%, which are mainly distributed in South China, North China, Southwest China, and Northwest China, such as Guangxi (32.8%), Beijing (34.5%), Guizhou (32.7%), and Gansu (33.2%). About 30% of the regions had OM fraction below 30.0%, mainly distributed in central and eastern China, such as Jiangsu (26.4%) and Hubei (29.0%). Compared with SNA and OM, the BC fractions of all provinces were lower than 10%, among which Hainan had the highest BC fraction (8.2%) and Anhui had the lowest BC fraction (5.5%).

### Trend analysis in the $PM_{2.5}$ chemical composition

Figure 5 summarizes the interannual trend of the average concentration of  $PM_{2.5}$  and its chemical components in China from 2000 to 2019. We can clearly find that the average concentration trend of  $PM_{2.5}$  and its chemical components in China presented an inverted U-shaped in the past 20 years. Before 2007, the average concentrations of  $PM_{2.5}$ , OM, BC,  $SO_2-4$ ,  $NO_3-3$  and  $NH_4+4$  increased at an annual rate of 1.74, 0.49, 0.12, 0.43, 0.46 and  $0.37 \mu g/m^3/yr$ , respectively. From 2008 to 2013, the average concentrations of  $PM_{2.5}$  ( $-0.08 \mu g/m^3/yr$ ), OM ( $-0.26 \mu g/m^3/yr$ ), BC ( $-0.08 \mu g/m^3/yr$ ),  $SO_2-4$  ( $-0.12 \mu g/m^3/yr$ ), and  $NH_4+4$  ( $-0.01 \mu g/m^3/yr$ ) in China began to decline slowly, while  $NO_3-3$  ( $0.06 \mu g/m^3/yr$ ) kept a slow increasing trend. After 2014, the average concentrations of  $PM_{2.5}$  and its chemical components showed a significant downward trend. In summary, from 2000 to 2019, the average concentrations of  $PM_{2.5}$ , OM, BC,  $SO_2-4$ , and  $NH_4+4$  decreased significantly at a rate of change of 0.59, 0.23, 0.07,



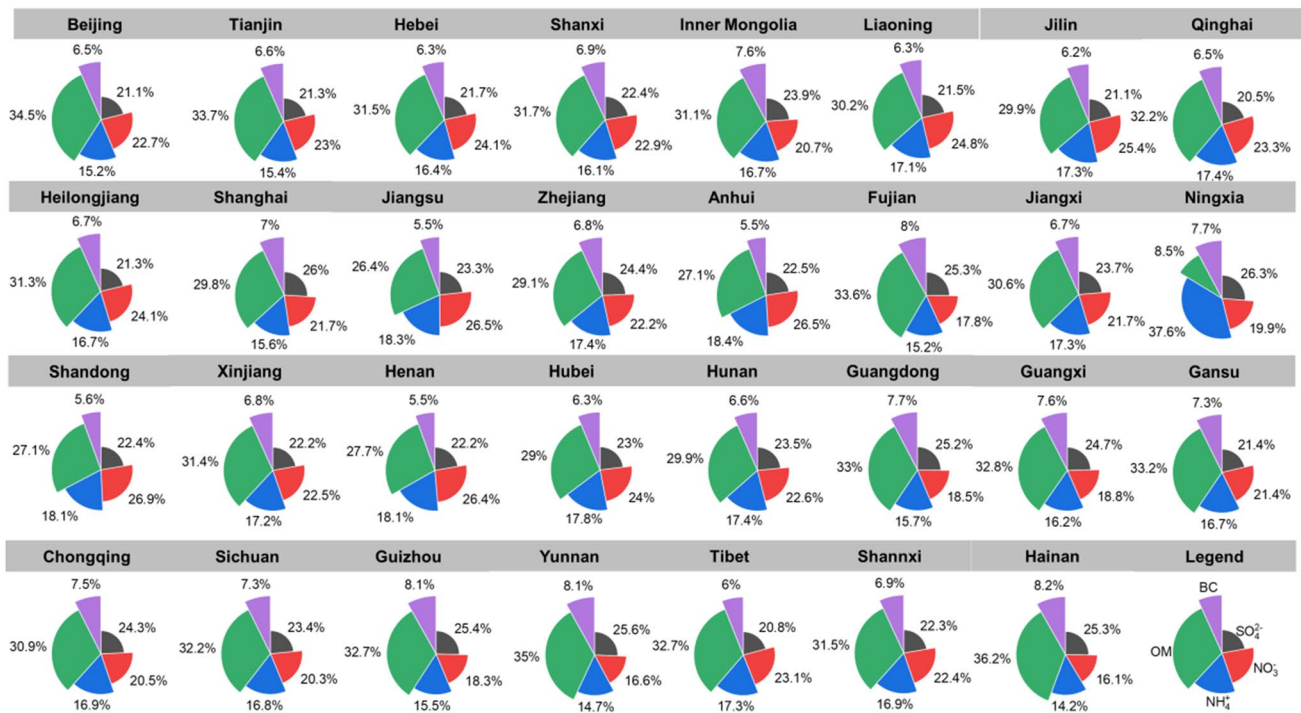


Fig. 4 The average PM<sub>2.5</sub> speciation for 31 provinces across China from 2000 to 2019

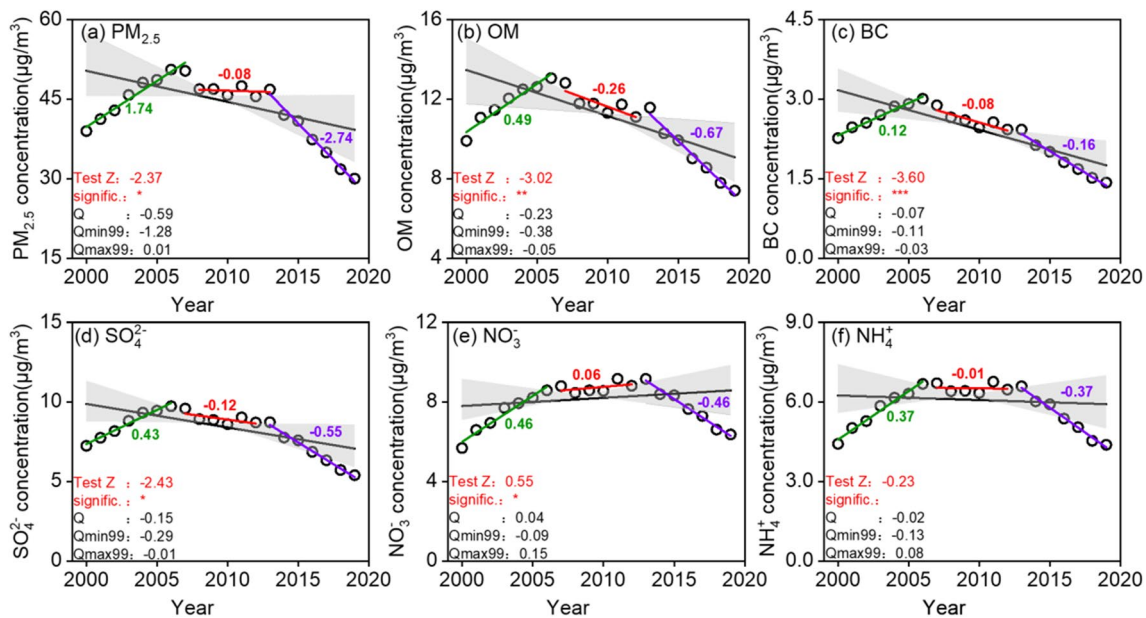


Fig. 5 Time series and trends in PM<sub>2.5</sub> (a), OM (b), BC (c), SO<sub>4</sub><sup>2-</sup> (d), NO<sub>3</sub><sup>-</sup> (e), and NH<sub>4</sub><sup>+</sup> (f) concentration from 2000 to 2019. The Qmax99 and Qmin99 indicate the lower and upper limits of the 99 % confidence interval of Q (i.e., gray areas), respectively. The solid

black, green, red, and purple lines indicate the fitting trends of different time intervals from 2000 to 2019, 2000 to 2007, 2008 to 2013, and 2014 to 2019, respectively. +, \*, \*\*, and \*\*\* indicate the significance level at 0.1, 0.05, 0.01, and 0.001, respectively

0.15, and 0.02µg/m<sup>3</sup>/yr, respectively. In contrast, NO<sub>3</sub><sup>-</sup> concentrations increased slightly at 0.04µg/m<sup>3</sup>/yr. More remarkably, however, the PM<sub>2.5</sub> component concentrations

maintained a substantial downward trend in China beyond 2019, which is associated with the strict lockdown imposed during the COVID-19 pandemic.

Figure 6 and Table.S2 show the spatial distribution of the interannual trend of  $PM_{2.5}$  and the concentration of its components in China from 2000 to 2019. For  $PM_{2.5}$  concentrations, there was a significant decrease in interannual trends in about 87% of provinces. The areas of significant decline were mainly distributed in Shanghai ( $-2.01\mu\text{g}/\text{m}^3/\text{yr}$ ), Beijing ( $-1.88\mu\text{g}/\text{m}^3/\text{yr}$ ), Tianjin ( $-1.74\mu\text{g}/\text{m}^3/\text{yr}$ ), Jiangsu ( $-1.10\mu\text{g}/\text{m}^3/\text{yr}$ ), Guangdong ( $-1.07\mu\text{g}/\text{m}^3/\text{yr}$ ), Henan ( $-1.05\mu\text{g}/\text{m}^3/\text{yr}$ ), and Shandong ( $-1.01\mu\text{g}/\text{m}^3/\text{yr}$ ), with an interannual trend of more than  $-1.0\mu\text{g}/\text{m}^3/\text{yr}$ . In contrast, the concentrations of  $PM_{2.5}$  in Gansu ( $0.01\mu\text{g}/\text{m}^3/\text{yr}$ ), Jilin ( $0.03\mu\text{g}/\text{m}^3/\text{yr}$ ) and Heilongjiang ( $0.17\mu\text{g}/\text{m}^3/\text{yr}$ ) showed a slightly increased trend. Similarly, the areas of significant  $SO_2-4$  decline were also distributed in Shanghai ( $-0.45\mu\text{g}/\text{m}^3/\text{yr}$ ), Tianjin ( $-0.41\mu\text{g}/\text{m}^3/\text{yr}$ ), Beijing ( $-0.34\mu\text{g}/\text{m}^3/\text{yr}$ ), Shandong ( $-0.27\mu\text{g}/\text{m}^3/\text{yr}$ ), Henan ( $-0.27\mu\text{g}/\text{m}^3/\text{yr}$ ), and Jiangsu ( $-0.23\mu\text{g}/\text{m}^3/\text{yr}$ ). For  $NO_3$ , only 9 provinces in

the country showed a significant decline, and the remaining 22 provinces increased to varying degrees. Among them, the largest increase and decrease in  $NO_3$  concentrations occurred in Hunan ( $0.21\mu\text{g}/\text{m}^3/\text{yr}$ ) and Tianjin ( $-0.15\mu\text{g}/\text{m}^3/\text{yr}$ ), respectively. The decrease in  $NH_4^+$  concentration was significant in East China, and the increase was relatively significant in Central China and Southwest China. The interannual trends of OM and BC concentrations showed similar spatial distributions, and the significant decline areas were mainly concentrated in Beijing (OM:  $-0.78\mu\text{g}/\text{m}^3/\text{yr}$ , BC:  $-0.16\mu\text{g}/\text{m}^3/\text{yr}$ ), Tianjin ( $-0.70\mu\text{g}/\text{m}^3/\text{yr}$ ,  $-0.16\mu\text{g}/\text{m}^3/\text{yr}$ ), Shanghai ( $-0.64\mu\text{g}/\text{m}^3/\text{yr}$ ,  $-0.16\mu\text{g}/\text{m}^3/\text{yr}$ ), Shandong ( $-0.42\mu\text{g}/\text{m}^3/\text{yr}$ ,  $-0.12\mu\text{g}/\text{m}^3/\text{yr}$ ), Jiangsu ( $-0.37\mu\text{g}/\text{m}^3/\text{yr}$ ,  $-0.10\mu\text{g}/\text{m}^3/\text{yr}$ ), and Hebei ( $-0.32\mu\text{g}/\text{m}^3/\text{yr}$ ,  $-0.09\mu\text{g}/\text{m}^3/\text{yr}$ ) in North China, East China, and Central China, and the areas with significant increases were distributed in Qinghai ( $0.05\mu\text{g}/\text{m}^3/\text{yr}$ ,  $0.01\mu\text{g}/\text{m}^3/\text{yr}$ ).

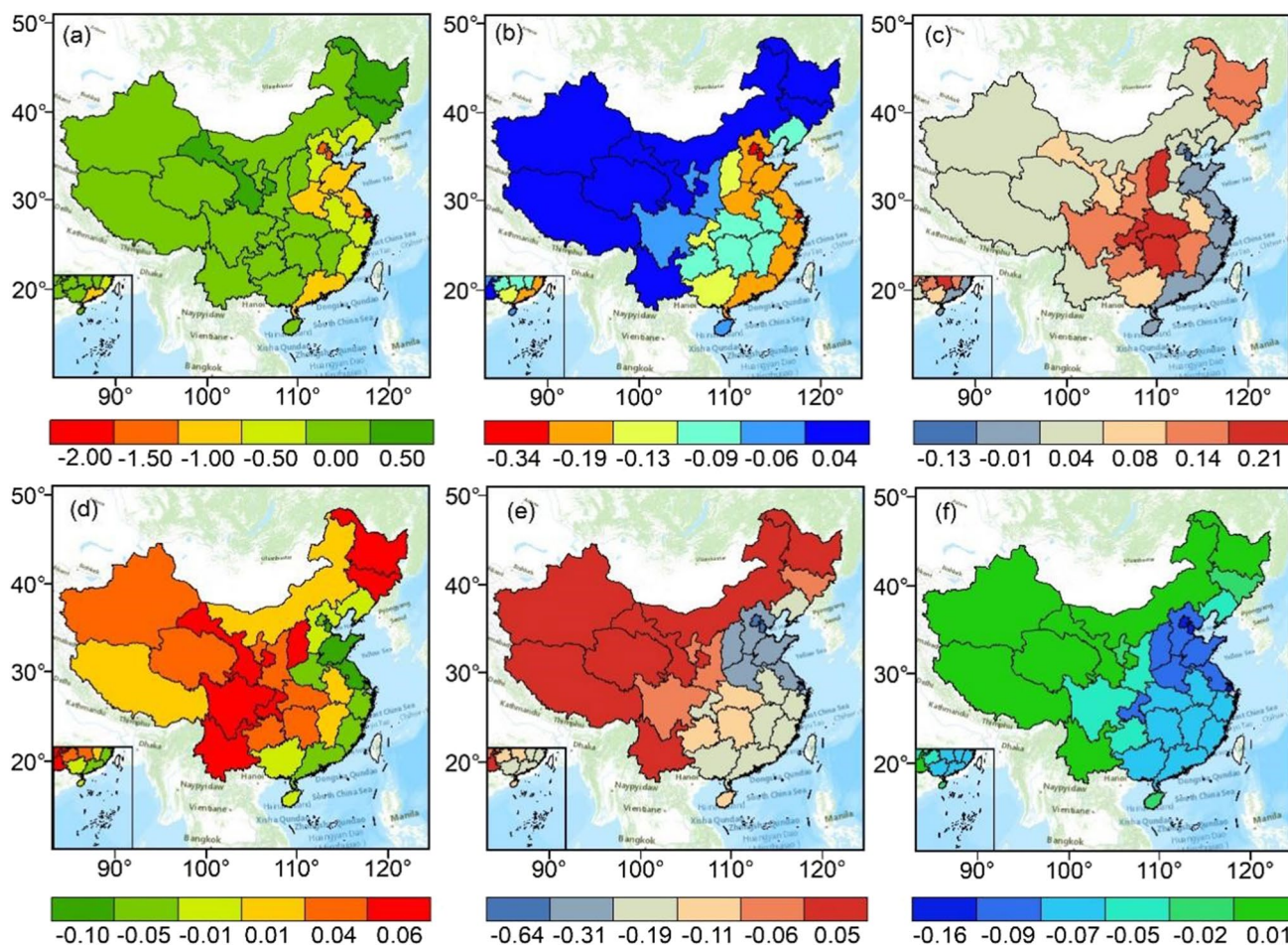


**Fig. 6** Spatial distributions of interannual trends in  $PM_{2.5}$  (a),  $SO_2-4$  (b),  $NO_3$  (c),  $NH_4^+$  (d), OM (e), and BC (f) concentrations in China from 2000 to 2019. The negative or positive trends were all

significant at the 99% confidence level after testing ( $p < 0.05$ ). The units for the trends in  $PM_{2.5}$ ,  $SO_2-4$ ,  $NO_3$ ,  $NH_4^+$ , OM, and OC concentration are all in  $\mu\text{g}/\text{m}^3/\text{year}$



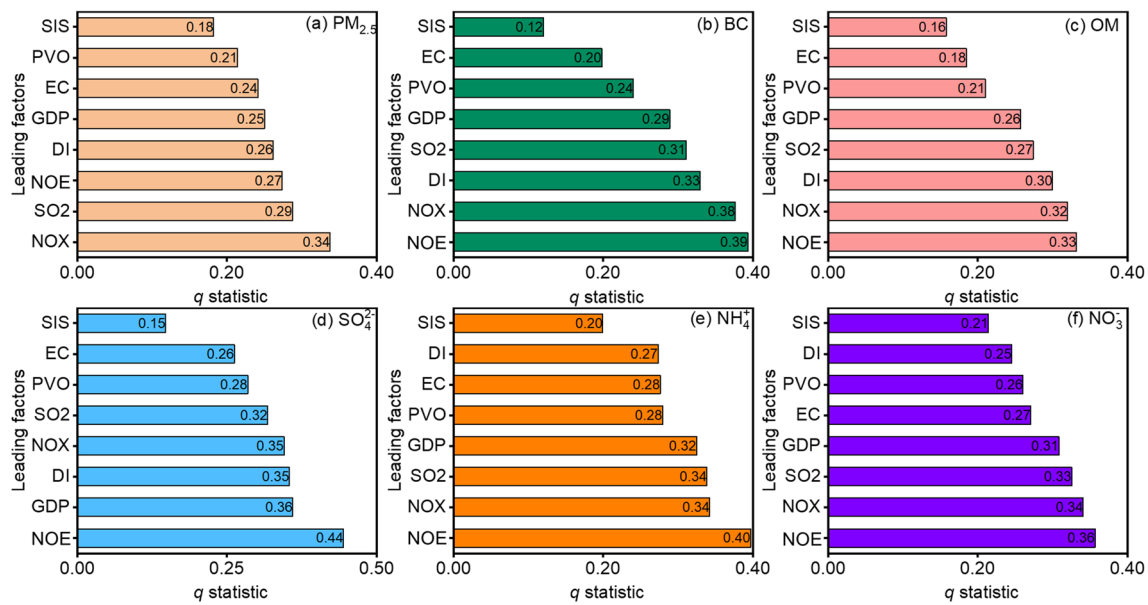


Fig. 7 The  $q$  value of  $PM_{2.5}$  component impact factor detection

### Drivers of the variation in $PM_{2.5}$ fraction concentration

Factor detection results ( $q$  values) reflect the degree of influence of factors on the spatial differentiation of  $PM_{2.5}$  components in China. For  $PM_{2.5}$  concentrations, NOx emissions have the highest  $q$  value ( $q=0.34$ ), which indicates that NOx emissions are the most dominant environmental factor determining the spatial pattern of  $PM_{2.5}$  emissions in China among these variables. The influence of  $SO_2$  emissions ( $q=0.29$ ) and the number of enterprises ( $q=0.27$ ) on the spatial pattern of  $PM_{2.5}$  emissions are followed by that of NOx emissions (Fig. 7a). With respect to concentration, OM,  $SO_2-4$ ,  $NH_4^+$ , and  $NO_3^-$  concentration, the number of enterprises is the most dominant socio-environmental factor affecting their spatial emission patterns, because the number of enterprises has the highest  $q$  values among all variables, with 0.39, 0.33, 0.44, 0.40, and 0.36, respectively. Additionally, NOx emissions ( $0.32 < q < 0.38$ ), population density ( $0.25 < q < 0.35$ ), GDP ( $0.26 < q < 0.36$ ), and  $SO_2$  emissions ( $0.27 < q < 0.34$ ) play an important role on the spatial pattern of the emission of BC, OM,  $SO_2-4$ ,  $NH_4^+$  and  $NO_3^-$  concentration emissions (Fig. 7b–f).

To further investigate the level of influence of the interaction factor on the spatial heterogeneity of  $PM_{2.5}$  component concentrations, this study used an interaction detector to reveal the interaction effect between the two drivers. The results of the interaction probe show that the explanatory power of the interaction between any two drivers on the spatial heterogeneity of  $PM_{2.5}$  fraction concentrations shows a two-factor enhancement or non-linear enhancement. It is

also found that the interaction effect of any two drivers on  $PM_{2.5}$  fractions is greater than the effect of individual drivers (Fig. 8 and Fig.S1). Specifically, the three critical interaction factors with the highest extent of influence on  $PM_{2.5}$  spatial heterogeneity are  $NOE \cap DI$  (note: the symbol  $\cap$  indicates the interaction between different socioeconomic factors),  $DI \cap EC$ , and  $PVO \cap SIS$ , with explanatory coefficients of 0.66, 0.70, and 0.67, respectively (Fig. 8a).  $NOE \cap DI$ ,  $DI \cap EC$ , and  $DI \cap SO_2$  are the three primary critical interaction factors with non-linear enhancement on BC spatial heterogeneity, with explanatory coefficients of 0.68, 0.69, and 0.70 (Fig. 8b). The three major key interaction factors with the highest degree of influence on OM spatial heterogeneity are  $NOE \cap DI$ ,  $DI \cap EC$ , and  $PVO \cap DI$ , with explanatory coefficients of 0.71, 0.74, and 0.68, respectively (Fig. 8c).  $NOE \cap DI$ ,  $NOE \cap SIS$ , and  $NOE \cap SO_2$  are the three main key interaction factors with non-linear enhancement on the spatial heterogeneity of  $SO_2-4$ , all with an explanatory power of 0.68 (Fig. 8d). The three critical interaction factors with the highest degree of influence on the spatial heterogeneity of  $NH_4^+$  are  $SIS \cap PVO$ ,  $SIS \cap NOE$ , and  $SO_2 \cap NOE$ , with explanatory powers of 0.73, 0.67, and 0.67, respectively, and they have non-linear enhancement on the spatial variation of  $NH_4^+$  concentration spatial heterogeneity with a non-linear enhancement effect (Fig. 8e). The  $NO_3^-$  spatial heterogeneity was most affected by the interactions of  $SIS \cap PVO$ ,  $SIS \cap NOE$ , and  $SO_2 \cap NOE$  with the explanatory coefficients of 0.73, 0.68, and 0.65, respectively (Fig. 8f).

Figure 9 shows the spatial distribution of cluster results in each province, and the heat map shows the values of each of the seven driving types. We can use Fig. 9 to understand

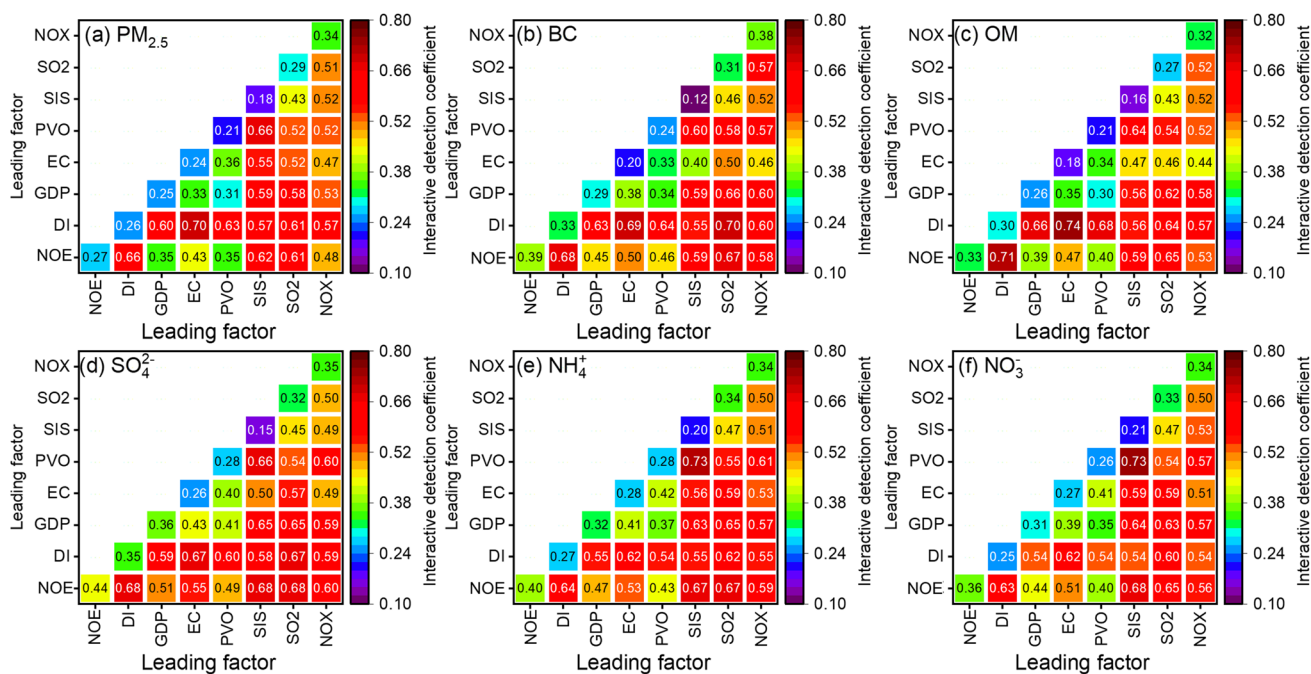


**Fig. 8** The  $q$  value of interaction detection between influencing factors

the spatial distribution of each province type and the specific drivers that province is most influenced by. For  $PM_{2.5}$  concentrations, EC was the most significant driver of  $PM_{2.5}$  concentrations in the C1 (NC), C3 (SW), and C4 (EC) regions with regression coefficients of 0.67, 1.16, and 0.77, respectively, and GDP (0.64) was the most important factor that affected the  $PM_{2.5}$  concentrations in the C2 (NW and CC) region, followed by EC (0.42) (Fig. 9a). For BC concentrations, EC was the largest driver affecting BC concentrations in the C1 (Most regions in China), C2 (NC), C3 (NE), and C4 (EC) regions with regression coefficients of 0.70, 0.93, 1.40, and 0.86, respectively (Fig. 9b). Similarly, EC was also the most dominant driver of OM concentrations in the C1 (most regions in China), C2 (NC), C3 (EC), and C4 (NE) regions with regression coefficients of 0.43, 0.95, 0.97, and 0.89, respectively (Fig. 9c). For  $NH_4^+$  concentrations, EC had a significantly higher effect on  $NH_4^+$  concentrations in the C1 (NW) and C4 (SW) regions with regression coefficients of 0.51 and 1.13, respectively. In contrast,  $SO_2$  emissions (0.20) and GDP (0.85) had the largest effect on  $NH_4^+$  concentrations in the C2 (NC and NE) and C3 (CC) regions (Fig. 9d). For  $NO_3$  concentrations, GDP was the largest influence on  $NO_3$  concentrations in the C2 (NW and CC) and C3 (SW) regions with regression coefficients of 0.85 and 0.60, respectively;  $SO_2$  emissions were the primary driver of  $NO_3$  concentration changes in the C1 (NC and NE) and C4 (EC) regions (Fig. 9e). For  $SO_2$  concentrations, EC was the most important driver affecting the change of  $SO_2$  concentrations in C2 (NC and NE),

C3 (EC), and C4 (SW) regions, while GDP was the primary factor affecting the change of  $SO_2$  concentrations in C1 (NW and CC) region (Fig. 9f).

## Discussion

### Spatial pattern of $PM_{2.5}$ chemical components

The spatial distribution of  $PM_{2.5}$  chemical components has a clear high-concentration area. These areas are mainly concentrated in the economically developed, populous, and industrially dense areas of Beijing-Tianjin-Hebei (BTH), Central China, and East China. Jin et al. (2017) showed that these regions become hotspots of  $PM_{2.5}$  pollution in China, which is related to the huge energy consumption and special geographical location. For example, BTH, as a major industrial agglomeration in China, has an energy consumption of about 0.56 tons of standard coal equivalent per 10,000 yuan of regional GDP in 2017 only which is significantly higher than the national average. Furthermore, some regions in BTH, have frequent unfavorable meteorological conditions (stable atmospheric section, smaller wind speed, etc.) due to their special geographical location, which suppress the horizontal transport and vertical diffusion of atmospheric pollutants and exacerbate the deterioration of the regional atmospheric environment (Cheng et al. 2016; He et al. 2017). Our study also found that SNA accounted for more than 50% of  $PM_{2.5}$  in all study areas, which was

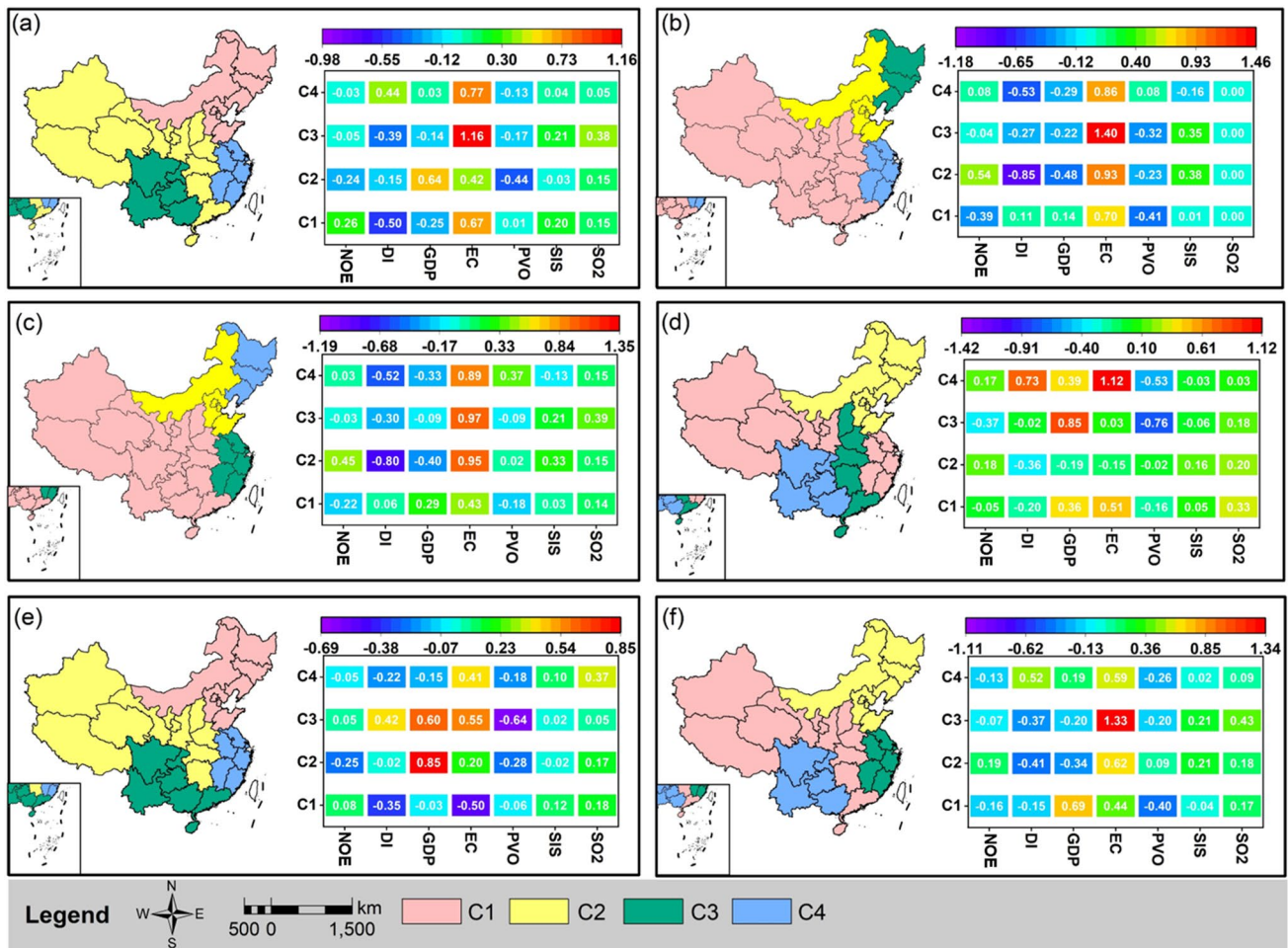


**Fig. 9** Four types of provinces obtained by clustering of the MGWR coefficients. Here, the map represents the spatial distribution of the clustering results of the dependent variables PM<sub>2.5</sub> (a), BC (b), OM

(c), NH<sub>4</sub><sup>+</sup> 4 (d), NO<sub>3</sub><sup>-</sup> 3 (e), and SO<sub>2</sub><sup>-</sup> 4 (f), and the heat map represents the clustering results of the MGWR coefficient

similar to the findings of Geng et al. (2017) and Ma et al. (2019) who suggested that SNA in PM<sub>2.5</sub> are readily generated in the atmosphere through secondary transformation of gaseous pollutants and were the most important components of atmospheric particulate matter, as well as the signature products of secondary atmospheric pollution.

**Trend variations of PM<sub>2.5</sub> chemical fraction**

The results of trend analysis showed that the trend of PM<sub>2.5</sub> chemical fraction in China was inverted U-shaped with strong spatial variation. Before 2013, the coal-based energy structure and the rough economic development model in China were the main reasons for the intensification of PM<sub>2.5</sub> pollution and the continuous increase of the corresponding chemical fraction in China. Previous studies have shown that fossil energy accounted for 86.2% of China’s energy consumption structure until 2013, while other energy accounts for only 13.8%. The intensive

consumption of fossil energy exacerbates the emission of pollutants such as soot, SO<sub>2</sub>, NO<sub>x</sub>, CO, and VOCs, further contributing to the degradation of air quality in China. Additionally, the high energy consumption per unit of GDP in China’s economic development process is also an important factor in the frequent occurrence of air pollution episodes (Cheng et al. 2021; Wang et al. 2020). This coal-based energy consumption emits a large amount of soot, SO<sub>2</sub>, NO<sub>x</sub>, CO, VOCs, and many other pollutants, which brings serious air pollution problems to China. Furthermore, China is characterized by a large economic volume and high energy consumption per unit of GDP. Economic growth often relies on increasing the amount of inputs of production factors to expand the scale of production. Under such circumstances, China’s air pollutant emissions approach or even exceed the environmental carrying capacity, which, combined with unfavorable meteorological conditions, has led to frequent air pollution events on a large scale and in multiple regions (Ming et al. 2017).



The dominant factor that shows a significant decrease in  $PM_{2.5}$  concentrations and component concentrations in China after 2013 is the emission reduction. Especially, after China promulgated and implemented the Action Plan for the Prevention and Control of Air Pollution in 2013, the emission of sulfur dioxide, nitrogen oxides, and primary  $PM_{2.5}$  in China was reduced by 16.4 million tons, 8 million tons, and 3.5 million tons, respectively, which resulted in a significant decrease in the exposure level of  $PM_{2.5}$  concentration for the Chinese population. In particular, the population-weighted annual average  $PM_{2.5}$  concentrations in the BTH, Yangtze River Delta (YRD), and Pearl River Delta (PRD) regions decreased from 102.8, 67.1, and 47.8  $\mu\text{g}/\text{m}^3$  in 2013 to 66.1, 44.0, and 34.4  $\mu\text{g}/\text{m}^3$  in 2017, respectively (Geng et al. 2017). Meanwhile, the trend analysis found that the  $PM_{2.5}$  fraction concentration remained on a substantial downward trend after 2019 in China, the most important reason being the strong nationwide blockade measures implemented by the Chinese government to combat the rapid spread of the virus after the COVID-19 outbreak. The unprecedented cessation of human activities led to a slowdown or even a standstill in industrial production, which inevitably resulted in a reduction in energy consumption, carbon emissions and industrial pollution (He et al. 2021). For example, He et al. (2020) found that the Chinese government's lockdown measures during COVID-19 resulted in a 19.84% decrease in air quality index (AQI) and a 14.07  $\mu\text{g}/\text{m}^3$  decrease in  $PM_{2.5}$  concentration in cities where the lockdown policy was implemented.

### Spatial heterogeneity of $PM_{2.5}$ chemical component emission drivers

The results of factor detection and interaction detection of the GD model show that different explanatory variables have effects on  $PM_{2.5}$  component emissions to different extents. Among all explanatory variables, the effect of the NOE on  $PM_{2.5}$  component emissions is significantly higher than other factors. This is because the NOE is an indicator that responds to the regional industrial level. The industrial level played an important supporting role in social and national economic development. However, production emissions from the industrial sector are one of the major sources of air pollution in China, and controlling industrial emissions poses a major challenge to air pollution control in China. Li et al. (2019) quantitatively evaluated the socioeconomic drivers of  $PM_{2.5}$  spatial and temporal variation in China using a spatial econometric approach based on the  $PM_{2.5}$  remote sensing inversion dataset from 1998 to 2013, and the results showed that industrial structure is considered to be one of the most important influencing factors on  $PM_{2.5}$  spatial variation. The second industry, especially heavy industries such as steel and cement, causing serious pollution has been a key concern of

the Chinese government in the last decade or so. Therefore, one of the effective measures to reduce  $PM_{2.5}$  pollution is to adjust and optimize the industrial structure. Similarly, Yang et al. (2023) investigated the spatial and temporal evolution and drivers of  $PM_{2.5}$  in key urban agglomerations in China based on a GD model, and they found similar results. These further suggested that industrial restructuring has an important role in future  $PM_{2.5}$  emission reduction in China.

In addition, the influence of NOE with DI, PVO, and SIS and interaction effects on  $PM_{2.5}$  component emissions are more pronounced, as the superimposed effects of multiple factors closely related to air pollution can exacerbate air pollution levels. A recent study showed that the air pollution levels in the industrial area of Wuhan Optics Valley are significantly higher than those in the Yang Luo Industrial Zone, although they are both important industrial centers in Wuhan, yet the Wuhan Optics Valley area is also an important transportation junction with significantly higher traffic flow than the Yang Luo area. This resulted in higher air pollution levels for similar industrial emission levels, under the influence of higher traffic emissions (Liang et al. 2016).

Based on the results of the MGWR model, we observe that GDP and  $\text{SO}_2$  emissions have the strongest impact on  $PM_{2.5}$ ,  $\text{NO}_3$ , and  $\text{SO}_2$  in North and East China. This can be attributed to the fact that these two regions produced more  $PM_{2.5}$  emissions than other regions during the economic development process. Meanwhile, this further indicated the potential association between these economic indicators and  $PM_{2.5}$  pollution. Additionally, these regions had a substantial potential to reduce  $PM_{2.5}$  emissions in terms of economic development and industrial level (Ou et al. 2022; Xu and Lin, 2016). EC had a significant impact on  $\text{NH}_4$  emissions in northwest China and BC and OM emissions in northeast China. The Northeast region was a major industrial center in China, and a substantial amount of industrial production was supported by large amounts of electrical energy. In addition, the Northwest and Northeast regions were among the coldest regions in China in winter and demand large amounts of electrical energy for domestic heating each year. The current electricity supply in Northeast and Northwest China is still dominated by thermal power generation, and the rapid increase of electric energy often requires the consumption of large amounts of fossil fuels, which will indirectly lead to  $\text{NH}_4$ , BC, and OM emissions in these regions (Han et al. 2011; Wang et al. 2018).

### Research limitations and future prospects

Our research results reveal the spatial and temporal evolution characteristics and driving factors of  $PM_{2.5}$  fraction concentrations to a certain extent. However, there are some limitations and shortcomings in this study: first, due to the lack of monitoring data from urban and background sites,

this study has not discussed the variation of PM<sub>2.5</sub> fraction concentrations between urban and background sites and its causes in detail. Actually, there is a significant over-variation of PM<sub>2.5</sub> fraction concentrations between urban and background sites due to the difference in population density, income status, and industrial structure. Second, this study only explores the spatial and temporal patterns and drivers of PM<sub>2.5</sub> fraction concentrations at the provincial scale, with no further in-depth investigation of PM<sub>2.5</sub> fraction concentration evolution patterns and their influencing factors at the municipal or grid scale. Third, the population exposure risk caused by air pollution is the most interesting hot issue currently. Although this study describes this issue to some extent in the introduction section, but the population exposure risk problem caused by the change of PM<sub>2.5</sub> component concentration is not quantitatively assessed.

In the future study, we hope to integrate the site monitoring data and reanalysis data to reveal the urban-rural variation characteristics of PM<sub>2.5</sub> fraction concentrations and population exposure risk from municipal or grid-scale using cross-method models such as environmental science, geographic information system (GIS), and epidemiology. This will provide key scientific support for authorities to implement regional air pollution control measures and reduce population exposure risk.

## Conclusions

In this study, we quantitatively analyzed the spatial patterns, trends, and key influencing factors of PM<sub>2.5</sub> chemical component concentrations in China utilizing the spatial analysis and spatial regression models based on the PM<sub>2.5</sub> chemical fraction concentration dataset from 2000 to 2019. The principal conclusions are as follows: the 20-year average concentrations of PM<sub>2.5</sub>, SO<sub>2</sub>–4, NO–3, NH<sub>4</sub>+4, OM and BC had significant spatial heterogeneity. The higher concentrations of PM<sub>2.5</sub>, SO<sub>2</sub>–4, NO–3, NH<sub>4</sub>+4, OM, and BC were mainly distributed in BTH, Central China, and East China. SNA had the highest fraction in PM<sub>2.5</sub> concentrations (55.6–68.1% in different provinces), followed by OM and BC, which accounted for 26.4–36.1 and 5.5–8.2% of PM<sub>2.5</sub>, respectively. The trend analysis shows that the change rates of PM<sub>2.5</sub>, OM, BC, SO<sub>2</sub>–4, NH<sub>4</sub>+4 and NO–3 in the entirety of China were –0.59, –0.23, –0.07, –0.15, –0.02, and 0.04 μg/m<sup>3</sup>/yr, respectively, for the entire study period across China. Meanwhile, we found that the national mean PM<sub>2.5</sub>, OM, BC, SO<sub>2</sub>–4, and NH<sub>4</sub>+4 concentration increased from 2000 to 2006 and subsequently decreased from 2007 to 2019, and the changing rates varied greatly from province to province.

The results of the GD model indicated that the number of enterprises, disposable income, electricity consumption,

private vehicle ownership, and the share of secondary industry was the most important drivers of spatial differences in PM<sub>2.5</sub> fraction concentrations in China. Furthermore, the results of the MGWR revealed the spatial differences of each factor on PM<sub>2.5</sub> component concentrations. The factors of GDP and SO<sub>2</sub> emissions in North and East China have significantly stronger effects on PM<sub>2.5</sub>, NO–3, and SO<sub>2</sub>–4 than those in Northwest and Southwest China. Electricity consumption had the most significant effects on NH<sub>4</sub>+4 emissions in Northwest China and BC and OM emissions in Northeast China.

**Supplementary Information** The online version contains supplementary material available at <https://doi.org/10.1007/s11356-023-28913-y>.

**Author contribution** Chao He and Jiming Jin: conceptualization, methodology, software, data curation, writing original draft and editing, and supervision. Bin Li and Lu Zhang: visualization and investigation. Lijun Liu and Xusheng Gong: writing—review and editing. Haiyan Li: software and validation.

**Funding** The research leading to these results received funding from the Hubei Provincial Natural Science Foundation of China (2021CFB112).

**Data availability** The data used to support the results of this research are shown in the manuscript and available from the corresponding author upon request.

## Declarations

**Ethics approval** Not applicable.

**Consent to participate** All authors agree to participate.

**Consent for publication** All authors agree to the publication.

**Competing interests** The authors declare no competing interests.

## References

- Apte JS, Brauer M, Cohen AJ et al (2018) Ambient PM<sub>2.5</sub> reduces global and regional life expectancy. *Environ Sci Technol Lett* 5:546–551
- Chen Z, Chen D, Zhao C et al (2020) Influence of meteorological conditions on PM<sub>2.5</sub> concentrations across China: a review of methodology and mechanism. *Environ Int* 139:105558
- Cheng Z, Luo L, Wang S et al (2016) Status and characteristics of ambient PM<sub>2.5</sub> pollution in global megacities. *Environ Int* 89:212–221
- Cheng J, Tong D, Zhang Q, Liu Y et al (2021) Pathways of China's PM<sub>2.5</sub> air quality 2015–2060 in the context of carbon neutrality. *Natl Sci Rev* 8(12):nwab078
- Cohen AJ, Brauer M, Burnett R et al (2017) Estimates and 25-year trends of the global burden of disease attributable to ambient air pollution: an analysis of data from the Global Burden of Diseases Study 2015. *Lancet* 389:1907–1918
- Feng Z, Hu E, Wang X et al (2015) Ground-level O<sub>3</sub> pollution and its impacts on food crops in China: a review. *Environ Pollut* 199:42–48

- Fotheringham AS, Yang W, Kang W (2017) Multiscale geographically weighted regression (MGWR). *Ann Am Assoc Geogr* 107:1247–1265
- Geng G, Zhang Q, Tong D et al (2017) Chemical composition of ambient PM<sub>2.5</sub> over China and relationship to precursor emissions during 2005–2012. *Atmos Chem Phys* 17:9187–9203
- Geng G, Xiao Q, Liu S et al (2021) Tracking air pollution in China: near real-time PM<sub>2.5</sub> retrievals from multisource data fusion. *Environ Sci Technol* 55:12106–12115
- Gong X, Hong S, Jaffe DA (2018) Ozone in China: spatial distribution and leading meteorological factors controlling O<sub>3</sub> in 16 Chinese cities. *Aerosol Air Qual Res* 18:2287–2300
- Guo H, Cheng T, Gu X et al (2017) Assessment of PM<sub>2.5</sub> concentrations and exposure throughout China using ground observations. *Sci Total Environ* 601:1024–1030
- Han YJ, Kim SR, Jung JH (2011) Long-term measurements of atmospheric PM 2.5 and its chemical composition in rural Korea. *J Atmos Chem* 68:281–298
- He J, Gong S, Yu Y et al (2017) Air pollution characteristics and their relation to meteorological conditions during 2014–2015 in major Chinese cities. *Environ Pollut* 223:484–496
- He G, Pan Y, Tanaka T (2020) The short-term impacts of COVID-19 lockdown on urban air pollution in China. *Nat Sustain* 3(12):1005–1011
- He C, Hong S, Zhang L et al (2021) Global, continental, and national variation in PM<sub>2.5</sub>, O<sub>3</sub>, and NO<sub>2</sub> concentrations during the early 2020 COVID-19 lockdown. *Atmos Pollut Res* 12(3):136–145
- Jbaily A, Zhou X, Liu J et al (2022) Air pollution exposure disparities across US population and income groups. *Nature* 601:228–233
- Jin Q, Fang X, Wen B et al (2017) Spatio-temporal variations of PM<sub>2.5</sub> emission in China from 2005 to 2014. *Chemosphere* 183:429–436
- Lelieveld J, Evans JS, Fnais M et al (2015) The contribution of outdoor air pollution sources to premature mortality on a global scale. *Nature* 525:367–371
- Li D, Zhao Y, Wu R et al (2019) Spatiotemporal features and socioeconomic drivers of PM<sub>2.5</sub> concentrations in China. *Sustain* 11:1201
- Liang X, Li S, Zhang S et al (2016) PM<sub>2.5</sub> data reliability, consistency, and air quality assessment in five Chinese cities. *J Geophys Res* 121:10220–10236
- Liang Z, Zhao X, Chen J et al (2019) Seasonal characteristics of chemical compositions and sources identification of PM<sub>2.5</sub> in Zhuhai, China. *Environ Geochem Health* 41:715–728
- Liu Y, Paciorek CJ, Koutrakis P (2009) Estimating regional spatial and temporal variability of PM<sub>2.5</sub> concentrations using satellite data, meteorology, and land use information. *Environ Health Perspect* 117:886–892
- Liu Z, Gao W, Yu Y et al (2018) Characteristics of PM<sub>2.5</sub> mass concentrations and chemical species in urban and background areas of China: emerging results from the CARE-China network. *Atmos Chem Phys* 18:8849–8871
- Liu K, Qiao Y, Zhou Q (2021) Analysis of China's industrial green development efficiency and driving factors: research based on MGWR. *Int J Environ Res Public Health* 18:3960
- Liu S, Geng G, Xiao Q et al (2022) Tracking daily concentrations of PM<sub>2.5</sub> chemical composition in China since 2000. *Environ Sci Technol* 56:16517–16527
- Ma Z, Liu R, Liu Y, Bi J (2019) Effects of air pollution control policies on PM<sub>2.5</sub> pollution improvement in China from 2005 to 2017: a satellite-based perspective. *Atmos Chem Phys* 19:6861–6877
- Ming L, Jin L, Li J et al (2017) PM<sub>2.5</sub> in the Yangtze River Delta, China: chemical compositions, seasonal variations, and regional pollution events. *Environ Pollut* 223:200–212
- Oshan TM, Li Z, Kang W et al (2019) MGWR: a python implementation of multiscale geographically weighted regression for investigating process spatial heterogeneity and scale. *ISPRS Int J Geo Inf* 8:269
- Ou S, Wei W, Cai B et al (2022) Exploring the causes for co-pollution of O<sub>3</sub> and PM<sub>2.5</sub> in summer over North China. *Environ Monit Assess* 194:289. <https://doi.org/10.1007/s10661-022-09951-4>
- Partal T, Kahya E (2006) Trend analysis in Turkish precipitation data. *Hydrol Process* 20:2011–2026
- Qin H, Huang Q, Zhang Z et al (2019) Carbon dioxide emission driving factors analysis and policy implications of Chinese cities: combining geographically weighted regression with two-step cluster. *Sci Total Environ* 684:413–424
- Sun YL, Wang ZF, Du W et al (2015) Long-term real-time measurements of aerosol particle composition in Beijing, China: seasonal variations, meteorological effects, and source analysis. *Atmos Chem Phys* 15:10149–10165
- Tran DX, Pearson D, Palmer A et al (2022) Quantifying spatial non-stationarity in the relationship between landscape structure and the provision of ecosystem services: an example in the New Zealand hill country. *Sci Total Environ* 808:152126
- Wang JF, Zhang TL, Fu BJ (2016) A measure of spatial stratified heterogeneity. *Ecol Indic* 67:250–256
- Wang X, Tian G, Yang D et al (2018) Responses of PM<sub>2.5</sub> pollution to urbanization in China. *Energy Policy* 123:602–610
- Wang S, Xu L, Ge S et al (2020) Driving force heterogeneity of urban PM<sub>2.5</sub> pollution: evidence from the Yangtze River Delta, China. *Ecol Indic* 113:106210
- Wei J, Li Z, Lyapunov A et al (2021) Reconstructing 1-km-resolution high-quality PM<sub>2.5</sub> data records from 2000 to 2018 in China: spatiotemporal variations and policy implications. *Remote Sens Environ* 252:112136
- Xiao Q, Geng G, Cheng J et al (2021) Evaluation of gap-filling approaches in satellite-based daily PM<sub>2.5</sub> prediction models. *Atmos Environ* 244:117921
- Xu B, Lin B (2016) Regional differences of pollution emissions in China: contributing factors and mitigation strategies. *J Clean Prod* 112:1454–1463
- Xu H, Jia Y, Sun Z et al (2022) Environmental pollution, a hidden culprit for health issues. *Eco-Environment & Health* 1(1):31–45
- Yang H, Yao R, Sun P et al (2023) Spatiotemporal evolution and driving forces of PM<sub>2.5</sub> in urban agglomerations in China. *Int J Environ Res Public Health* 20:2316
- Yu FW, Chan KT (2012) Using cluster and multivariate analyses to appraise the operating performance of a chiller system serving an institutional building. *Energy Build* 44:104–113
- Zhao H, Gui K, Ma Y et al (2022) Multi-year variation of ozone and particulate matter in Northeast China based on the Tracking Air Pollution in China (TAP) data. *Int J Environ Res Public Health* 19:3830
- Zheng Y, Wen X, Bian J et al (2021) Associations between the chemical composition of PM<sub>2.5</sub> and gestational diabetes mellitus. *Environ Res* 198:110470

**Publisher's note** Springer Nature remains neutral with regard to jurisdictional claims in published maps and institutional affiliations.

Springer Nature or its licensor (e.g. a society or other partner) holds exclusive rights to this article under a publishing agreement with the author(s) or other rightsholder(s); author self-archiving of the accepted manuscript version of this article is solely governed by the terms of such publishing agreement and applicable law.